The Effect of Temperature on Physical Aging of Glassy Polymers

ALEKSEY D. DROZDOV

Institute for Industrial Mathematics, 4 Hanachtom Street, Beersheba, 84311 Israel

Received 27 October 2000; accepted 4 January 2001

ABSTRACT: Constitutive equations are derived for the linear viscoelastic response of amorphous glassy polymers subjected to physical aging. Stress–strain relations are applied to fit experimental data for poly(methyl methacrylate), poly(styrene-*co*-acronitrile), and poly(vinyl acetate) in tensile relaxation tests and in torsional dynamic tests at various temperatures. Fair agreement is demonstrated between observations and results of numerical simulation. It is revealed that an increase in the annealing temperature results in an increase in the rate of relaxation and a decrease in the apparent rate of structural recovery. © 2001 John Wiley & Sons, Inc. J Appl Polym Sci 81: 3309–3320, 2001

Key words: glassy polymers; viscoelasticity; physical aging; thermal effects; constitutive equations

INTRODUCTION

This paper is concerned with the effect of temperature on the kinetics of physical aging in amorphous glassy polymers. Physical aging (structural relaxation) in polymeric glasses has been a focus of attention in the past decade (see monographs[1–4] and review articles[5–8]). This phenomenon is conventionally studied in one-step thermal tests, where a specimen equilibrated at some temperature T_0 above the glass transition temperature T_g is quenched to a temperature $T < T_g$ and is isothermally annealed at the temperature T. Structural relaxation is evidenced as changes in specific volume, specific enthalpy, elastic moduli, relaxation (retardation) spectra, yield stress, etc. with waiting time (the time elapsed after quench before the beginning of the test).

The present study deals with mechanical tests, where an increase in the waiting time results in an increase in elastic moduli and relaxation (retardation) times. Following Struik,[9] physical aging of glassy polymers is traditionally described by means of the time–aging time principle of superposition. According to this postulate, relaxation (retardation) curves measured at various waiting times t_w and plotted on double logarithmic coordinates can be superposed by shifts along the horizontal (time) axis (with additional shifts along the vertical axis, if necessary). The horizontal shift, a_s, reflects changes in relaxation (retardation) times, whereas the vertical shift, b_s, characterizes evolution of elastic moduli with waiting time. Observations reveal that the dependence of the horizontal shift, a_s, on the waiting time, t_w, is correctly predicted by the phenomenological relation

$$\frac{\mathrm{d} \log a_s}{\mathrm{d} \log t_w} = \mu$$

where the constant μ (the rate of aging) is close to unity.

Correspondence to: A. D. Drozdov (aleksey@cs.bgu.ac.il).

Journal of Applied Polymer Science, Vol. 81, 3309–3320 (2001)

To explain an increase in relaxation (retardation) times with waiting time, the concept of molecular mobility is proposed.[9] According to this concept, annealing of a specimen at some temperature T below the glass transition point results in a decrease in mobility of segments of long chains. This effect is associated with a drop in free volume of polymeric glasses, which is confirmed by experimental data in dilatometric[9] and PALS[10–12] tests.

The following shortcomings of the time–aging time principle of superposition may be mentioned:

1. This postulate is based on the free volume concept,[13,14] which is poorly defined from the physical standpoint[15] and which totally neglects the thermal activation necessary for redistribution of free volume clusters.[16]
2. A molecular mechanism remains obscure for the evolution of free volume with waiting time.
3. A plausible model is absent for correlations between changes in free volume and alteration of relaxation spectra.
4. The superposition principle presumes that the ratios of relaxation (retardation) rates do not change with waiting time. Although this hypothesis substantially simplifies the analysis of experimental data, no arguments are provided for its justification.
5. Observations in dilatometric tests on loaded specimens evidence that the rate of decrease in the specific volume is independent of stresses,[17] which questions correlations between molecular mobility and free volume (at least, in the region of nonlinear viscoelasticity).
6. Experimental data for several amorphous polymers demonstrate poor superposition of relaxation curves (see ref. 18 and the references therein).
7. The assumption that the rate of aging μ is close to unity implies that the annealing temperature T weakly affects the kinetics of aging, which contradicts observations in dilatometric and calorimetric tests (see refs. 19–21 and 22–25, to mention a few).

This study focuses on the effect of annealing temperature on structural relaxation in polymeric glasses observed in mechanical tests. The objective is three-fold: (i) to develop a molecular model for physical aging in glassy polymers, (ii) to apply constitutive equations to the analysis of experimental data in static and dynamic tests on aged samples, and (iii) to demonstrate that the kinetics of structural recovery is noticeably affected by the aging temperature.

To derive a molecular model, we combine the theory of cooperative relaxation in amorphous polymers[26] with the coarsening concept for structural recovery in glasses after thermal treatment.[8] An amorphous polymer is treated as an ensemble of cooperatively rearranged regions (CRR) bridged by links. A CRR is thought of as a globule consisting of scores of neighboring strands[27] that change their position simultaneously because of large-angle reorientation of long chains[28] [observed, for example, by time–domain nuclear magnetic resonance (NMR) spectroscopy[29]]. The initiation of CRRs is associated with dynamic heterogeneity above the glass transition temperature, which results in the onset of temporary microdomains with high and low densities.[7,30,31] The presence of large-scale density fluctuations in polymeric liquids near the glass transition point has been confirmed by numerous experiments (see ref. 32 and the references therein). The characteristic length of a relaxing region in the vicinity of the glass transition temperature T_g amounts to several nanometers.[33–35] The size of a CRR increases with the degree of supercooling[33] ($\Delta T = T_g - T$) because of slow evolution of microdomains to an equilibrium state driven by their coarsening.[8] In the α-relaxation region, CRRs are identified with isolated "more cohesive regions" observed by low-frequency Raman scattering, whereas the bridges (links), between CRRs is thought of as "less cohesive spaces percolated through the material."[36] We do not make concrete the physical nature of links and associate them with physical and chemical crosslinks, entanglements, and van der Waals forces.

According to the trapping concept,[28,37] a CRR is modeled as a material point trapped at the bottom level of its potential well on the energy landscape. The applicability of the energy landscape theory to polymeric glasses is discussed by Roland et al.[38] At random times, a CRR hops to higher energy levels as the relaxing region is thermally agitated, but it cannot leave the trap (the pattern of ergodicity breaking[39]). With reference to the transition state theory,[40] it is assumed that some liquid-like (reference) energy level exists on the energy landscape, where CRRs change their configurations. When a CRR reaches the liquid-like state in a hop, stresses totally relax in it. If a relaxing region hops below the reference

level, it returns to its initial position in the potential well without changes.

The zero level on the energy landscape is introduced at the bottom level of a potential well with the minimal depth. The depth of any potential well with respect to the zero energy level is determined by its energy $w \geq 0$. The distribution of potential wells with various energies (depths) after annealing for a time t_w upon quench is described by the probability density $p(t_w, w)$. Adopting the coarsening concept,[8,41] we postulate that evolution of the distribution function $p(t_w, w)$ with waiting time t_w is driven by fragmentation and aggregation of neighboring regions. We do not dwell on the kinetics of coalescence, referring to the survey by Yoshino et al.[42] and the references therein. Results of numerical simulation (see ref. 43) demonstrate that at the initial stage of structural recovery, the distribution of CRRs, $p(t_w, w)$, may be adequately described by the exponential function

$$p(t_w, w) = \frac{1}{W(t_w)} \exp\left[-\frac{w}{W(t_w)}\right] \qquad (w \geq 0) \tag{1a}$$

$$p(t_w, w) = 0 \qquad (w < 0) \tag{1b}$$

where $W(t_w)$ is the mathematical expectation of energies of CRRs. The advantage of eqs. 1a and 1b is that for a given waiting time t_w, they contain only one adjustable parameter, $W(t_w)$, to be found by fitting experimental data in standard tests. The exponential distribution function has been previously suggested by Bouchaud,[37] without detailed explanations. Among other expressions for the function p, we would mention the Gaussian distribution[28] and the generalized Gaussian distribution.[44]

The exposition is organized as follows. The next section deals with stress-strain relations for an amorphous polymer at isothermal loading with small strain. The constitutive equations are verified by comparison with experimental data for poly(methyl methacrylate) (PMMA), poly(styrene-*co*-acronitrile) (SAN), and poly(vinyl acetate) (PVAc) at various degrees of supercooling. Some concluding remarks are formulated in the last section.

CONSTITUTIVE EQUATIONS

We focus on short-term mechanical tests, whose duration is essentially less than the waiting time t_w. The viscoelastic response of glassy polymers is modeled as a sequence of (driven by thermal fluctuations) random hops of rearranging regions in their potential wells.[45] Let $q(z)\,\mathrm{d}z$ be the probability for a CRR to reach (in a hop) the energy level that exceeds the bottom level of its potential well by a value belonging to the interval $[z, z + \mathrm{d}z]$. Referring to Bouchaud et al.,[8] we postulate that

$$q(z) = \alpha \exp(-\alpha z) \tag{2}$$

where α is a material constant. Denote by Ω the position of the liquid-like (reference) state with respect to the zero energy level. The probability for a relaxing region in a trap with energy w to reach the reference state in an arbitrary hop is given by

$$Q(w) = \int_{\Omega+w}^{\infty} q(z)\,\mathrm{d}z = \exp[-\alpha(\Omega + w)] \tag{3}$$

Let Γ_0 be the attempt rate (the average number of hops in a potential well per unit time). We assume that Γ_0 is independent of w and is determined by the current temperature T only. Multiplying the attempt rate, Γ_0, by the probability to reach the reference state in a hop, Q, we find the rate of rearrangement in a trap with potential energy w,

$$R(w) = \Gamma \exp(-\alpha w) \tag{4}$$

where

$$\Gamma = \Gamma_0 \exp(-\alpha\Omega) \tag{5}$$

is the rate of relaxation.

Denote by $\Xi_0(t_w)$ the number of CRRs in the ensemble of relaxing regions (per unit mass) after waiting for a time t_w upon quench. All regions are assumed to be rigidly connected by links with one another, which implies that the macrostrain in a specimen coincides with the microstrain in each CRR. Let $\Xi(t, \tau, w)$ be the current concentration of CRRs located in traps with potential energy w that has last been rearranged before instant $0 \leq \tau \leq t$. The initial instant, $t = 0$, coincides with the beginning of a test and corresponds to the waiting time t_w in the absolute time scale.

The function Ξ entirely determines the distribution of CRRs. In particular, $\Xi(t, 0, w)$ is the concentration of relaxing regions that have not

been rearranged until time t, $\Xi(t, t, w)$ is the current concentration of CRRs in potential wells with energy w, and $\partial\Xi/\partial\tau(t, \tau, w)\,d\tau$ is the number of relaxing regions at time t (per unit mass) that have last been rearranged within the interval $[\tau, \tau + d\tau]$. For short-term mechanical tests, the function Ξ obeys the condition

$$\Xi(t, t, w) = \Xi_0(t_w)p(t_w, w) \tag{6}$$

Evolution of the function Ξ is determined by rearrangement of relaxing regions (with the relative rate R), which implies that the functions $\Xi(t, 0, w)$ and $\partial\Xi/\partial\tau(t, \tau, w)$ satisfy the differential equations

$$\frac{\partial\Xi}{\partial t}(t, 0, w) = -R(w)\Xi(t, 0, w) \tag{7}$$

$$\frac{\partial^2\Xi}{\partial t\partial\tau}(t, \tau, w) = -R(w)\frac{\partial\Xi}{\partial\tau}(t, \tau, w) \tag{8}$$

The solution of these equations with the initial condition (eq. 6) reads

$$\Xi(t, 0, w) = \Xi_0(t_w)p(t_w, w)\exp[-R(w)t] \tag{9}$$

$$\frac{\partial\Xi}{\partial\tau}(t, \tau, w) = F(\tau, w)\exp[-R(w)(t - \tau)] \tag{10}$$

where

$$F(\tau, w) = \frac{\partial\Xi}{\partial\tau}(t, \tau, w)\Big|_{t=\tau} \tag{11}$$

The quantity $F(t, w)\,dt$ equals the number of CRRs with potential energy w (per unit mass) rearranged within the interval $[t, t + dt]$. To calculate this value, we sum the number of initial regions rearranged within this interval,

$$R(w)\Xi(t, 0, w)\,dt \tag{12}$$

and the number of CRRs relaxed at some instant $\tau \le t$ and reaching the reference state within the interval $[t, t + dt]$,

$$\int_0^t R(w)\frac{\partial\Xi}{\partial\tau}(t, \tau, w)\,d\tau\,dt \tag{13}$$

which results in the equality

$$F(t, w) = R(w)\left[\Xi(t, 0, w) + \int_0^t \frac{\partial\Xi}{\partial\tau}(t, \tau, w)\,d\tau\right] = R(w)\Xi(t, t, w) \tag{14}$$

Substitution of eq. 9 into this formula implies that

$$F(t, w) = \Xi_0(t_w)p(t_w, w)R(w) \tag{15}$$

which, together with eq. 10 results in the formula

$$\frac{\partial\Xi}{\partial\tau}(t, \tau, w) = \Xi_0(t_w)p(t_w, w) \times R(w)\exp[-R(w)(t - \tau)] \tag{16}$$

At uniaxial loading, a CRR is modeled as a linear elastic solid with the mechanical energy

$$\psi(t, \tau, w) = \tfrac{1}{2}c(t_w, w)\varepsilon^2(t, \tau) \tag{17}$$

where c is the rigidity of the CRR and ε is the strain from its natural (stress-free) state to the deformed state. Unlike previous studies (see refs. 46 and 47), we postulate that the rigidity of a CRR is proportional to its volume, v, which, in turn, is assumed to be proportional to the energy, w, of the potential well, where the relaxing region is trapped,

$$c(t_w, w) = c_0(t_w)w \tag{18}$$

where $c_0(t_w)$ is the average specific rigidity (per unit energy) of relaxing regions.

To explain the dependence of the specific rigidity on waiting time, we suppose that c_0 is determined by the current molecular configuration of a CRR. For a loose configuration, the rigidity is relatively small, and it substantially grows when the configuration becomes more compact. To simplify the analysis, it is postulated that only two configurations exist for a CRR, loose and tight, and the rigidity c_0 takes the value c_1 for the loose configuration and $c_2 > c_1$ for the tight one. These two configurations may be associated with two subwells of the potential well where a CRR is trapped on the energy landscape. A similar picture (a two-well potential) was suggested by Gibbs et al.[48] and, more recently, by Khonik[49] to

predict structural recovery in glasses. Immediately upon quench from above the glass transition temperature, the majority of CRRs are in loose configurations (with most strands located to trans states), which implies that the initial rigidity, $c_0(0)$, is rather small. With the growth of waiting time t_w, trans states of some CRRs are replaced by cis states, which is modeled as hops across an energy barrier separating the two subwells (whose height is determined by the difference between the energy of cis and trans states of strands performing this transformation).[50] As a result, the specific rigidity of a CRR, c_0, monotonically increases with waiting time t_w.

Because a CRR totally relaxes reaching the liquid-like state, its stress-free configuration coincides with the deformed configuration of the bulk material at the instant of rearrangement. This result implies that the strain ε from the stress-free configuration of a relaxing region to its deformed configuration at time t is given by

$$\varepsilon(t,\ \tau) = \epsilon(t) - \epsilon(\tau) \tag{19}$$

where ϵ is the microstrain in a CRR (which coincides with the macrostrain in a specimen). Combining eqs. 17–19, we obtain

$$\psi(t,\ \tau,\ w) = \tfrac{1}{2}\, c_0(t_w) w [\epsilon(t) - \epsilon(\tau)]^2 \tag{20}$$

The mechanical energy (per unit mass) of CRRs that have not been rearranged during the interval $[0,\ t)$ is given by

$$\frac{1}{2}\, c_0(t_w)\epsilon^2(t) \int_0^\infty \Xi(t,\ 0,\ w) w\ dw \tag{21}$$

and the mechanical energy of relaxing regions that rearranged within the interval $[\tau,\ \tau + \mathrm{d}\tau]$ and have not returned to the reference state until the current time t is calculated as

$$\frac{1}{2}\, c_0(t_w)[\epsilon(t) - \epsilon(\tau)]^2 \int_0^\infty \frac{\partial \Xi}{\partial \tau}\,(t,\ \tau,\ w) w\ \mathrm{d}w\ \mathrm{d}\tau \tag{22}$$

Summing these expressions and neglecting the energy of interaction between CRRs, we find the mechanical energy of an amorphous polymer (per unit mass)

$$\Psi(t) = \frac{1}{2}\, c_0(t_w)\left\{ \epsilon^2(t) \int_0^\infty \Xi(t,\ 0,\ w) w\ \mathrm{d}w + \int_0^t [\epsilon(t) - \epsilon(\tau)]^2\ \mathrm{d}\tau \int_0^\infty \frac{\partial \Xi}{\partial \tau}\,(t,\ \tau,\ w) w\ \mathrm{d}w \right\} \tag{23}$$

At small strains, the stress σ is expressed in terms of the mechanical energy per unit mass, Ψ, by the formula

$$\sigma(t) = \rho\, \frac{\partial \Psi(t)}{\partial \epsilon(t)} \tag{24}$$

where ρ is mass density in the stress-free state. Substitution of eq. 23 into eq. 24 implies the following stress-strain relation:

$$\sigma(t) = \rho c_0(t_w)\left[\epsilon(t) \int_0^\infty \Xi(t,\ 0,\ w) w\ \mathrm{d}w + \int_0^t (\epsilon(t) - \epsilon(\tau))\ \mathrm{d}\tau \int_0^\infty \frac{\partial \Xi}{\partial \tau}\,(t,\ \tau,\ w) w\ \mathrm{d}w \right] \tag{25}$$

Given a loading program, $\epsilon(t)$, constitutive eq. 25 is determined by the specific rigidity of a CRR, $c_0(t_w)$, and the concentration, $\Xi(t,\ \tau,\ w)$, of relaxing regions trapped in potential wells with energies w. The function $\Xi(t,\ \tau,\ w)$ is described by eqs. 9 and 16 where the rate of rearrangement, $R(w)$ is given by eq. 4.

We concentrate of two programs of loading, which are frequently used in experiments.

Relaxation Tests

For a standard relaxation test with

$$\epsilon(t) = \begin{cases} 0, & t < 0, \\ \epsilon_0, & t \geq 0 \end{cases} \tag{26}$$

where the strain ϵ_0 is essentially less than the yield strain, ϵ_y, eq. 25 implies that

$$\sigma(t) = E_0(t_w)\epsilon_0 \int_0^\infty p(t_w,\ w) \exp[-\Gamma t \exp(-\alpha w)]\ \mathrm{d}w \tag{27}$$

where

$$E_0(t_w) = \rho c_0(t_w)\Xi_0(t_w) \tag{28}$$

is the initial Young modulus (for definiteness, we consider tensile tests). Combining eqs. 1 and 28, we obtain

$$E(t) = E_0(t_w)\int_0^\infty \frac{w}{W(t_w)} \times \exp\left[-\left(\frac{w}{W(t_w)} + \Gamma t\exp(-\alpha w)\right)\right] dw \tag{29}$$

where $E(t) = \sigma(t)/\epsilon_0$ is the current Young modulus.

Dynamic Tests

For a dynamic test with the frequency ω, we set

$$\epsilon(t) = \begin{cases} 0, & t < 0, \\ \epsilon_0\exp(i\omega t), & t \geq 0 \end{cases} \tag{30}$$

where $i = \sqrt{-1}$. It follows from eqs. 25 and 30 that

$$\sigma(t) = E_0(t_w)\epsilon_0\exp(i\omega t) \times \left\{1 - \Gamma\int_0^\infty p(t_w, w)\exp(-\alpha w)w\, dw \times \int_0^t \exp[-(i\omega + \Gamma\exp(-\alpha w))(t-\tau)]\, d\tau\right\} \tag{31}$$

Combining eqs. 30 and 31 and introducing the notation

$$\sigma(t) = E^*\epsilon(t) \tag{32}$$

where E^* is the complex elastic modulus, we arrive at the formula

$$E^*(t_w, \omega) = E_0(t_w) \times \left\{1 - \Gamma\int_0^\infty p(t_w, w)\exp(-\alpha w)w\, dw \times \int_0^t \exp[-(i\omega + \Gamma\exp(-\alpha w))s]\, ds\right\} \tag{33}$$

where $s = t - \tau$. Replacing the upper limit of integration by infinity and calculating the integral, we find that

$$E^* = E_0(t_w)\left[1 - \Gamma\int_0^\infty \frac{p(t_w, w)\exp(-\alpha w)w}{\Gamma\exp(-\alpha w) + i\omega}\, dw\right] \tag{34}$$

The complex modulus E^* is presented in the form

$$E^* = E' + iE'' \tag{35}$$

where E' is the storage modulus and E'' is the loss modulus. It follows from eqs. 1 and 34 that

$$E'(t_w, \omega) = \frac{E_0(t_w)\omega^2}{W(t_w)}\int_0^\infty \frac{1}{\Gamma^2\exp(-2\alpha w) + \omega^2} \times \exp\left(-\frac{w}{W(t_w)}\right)w\, dw \tag{36}$$

$$E''(t_w, \omega) = \frac{E_0(t_w)\Gamma\omega}{W(t_w)}\int_0^\infty \frac{\exp(-\alpha w)}{\Gamma^2\exp(-2\alpha w) + \omega^2} \times \exp\left(-\frac{w}{W(t_w)}\right)w\, dw \tag{37}$$

Given a waiting time t_w, governing eqs. 29 and 37 are determined by three adjustable parameters: the initial Young modulus, E_0, the average dimensionless energy of a CRR, W, and the relaxation rate, Γ. Without loss of generality, we set $\alpha = 1$ [this quantity may be excluded from eqs. 29 and 37 by the transformation $\alpha w \to w$ and $\alpha W \to W$].

COMPARISON WITH EXPERIMENTAL DATA

To validate stress-strain relations, we fit observations in tensile relaxation tests for poly(methyl methacrylate) ($T_g = 106$°C) at various temperatures T. For a description of specimens and the experimental procedure, we refer to works by Mijovic and co-workers.[51,52] Equation 29 implies that the ratio of elastic moduli

$$r(t_w, t) = \frac{E(t)}{E_0(t_w)} \tag{38}$$

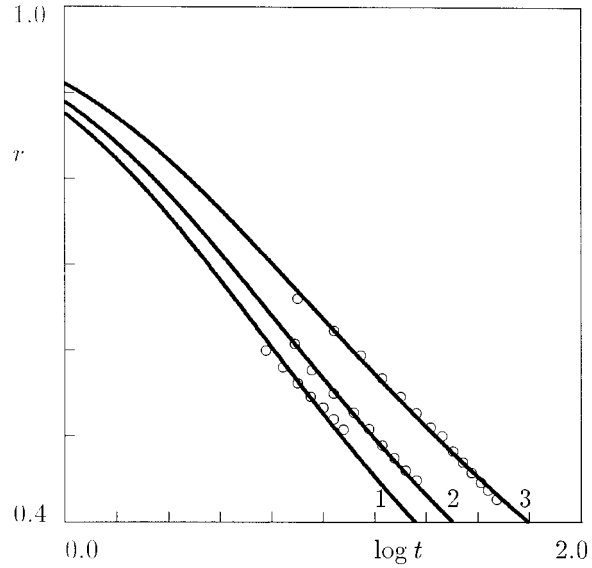

Figure 1 The ratio $r(t)$ versus time t (s) for PMMA in a tensile relaxation test after annealing at the temperature $T = T_g - 20$ K for a time t_w (h). Key: (circles) experimental data[51,52]; (solid lines) results of numerical simulation; (Curve 1) $t_w = 2.0$; (curve 2) $t_w = 4.0$; (curve 3) $t_w = 8.0$.

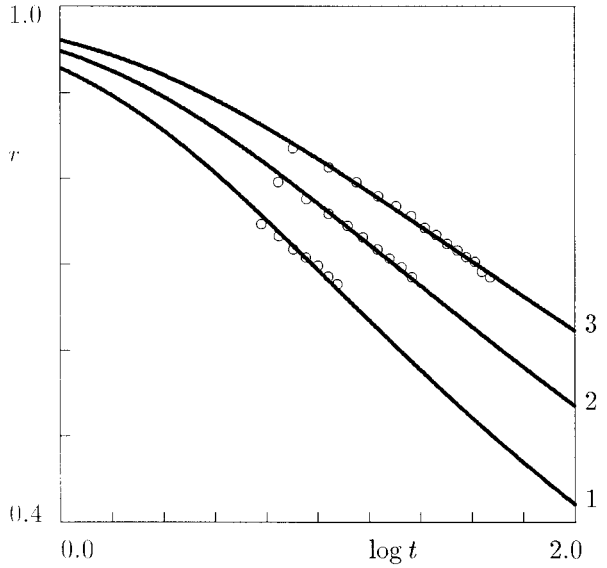

Figure 2 The ratio $r(t)$ versus time t (s) for PMMA in a tensile relaxation test after annealing at the temperature $T = T_g - 35$ K for a time t_w (h). Key: (circles) experimental data[51,52]; (solid lines) results of numerical simulation; (curve 1) $t_w = 2.0$; (curve 2) $t_w = 4.0$; (curve 3) $t_w = 8.0$.

is determined by two adjustable parameters, Γ and W:

$$r(t_w, t) = \int_0^\infty \frac{w}{W(t_w)} \times \exp\left[-\left(\frac{w}{W(t_w)} + \Gamma t \exp(-w)\right)\right] dw \quad (39)$$

We begin with matching observations in a test with the degree of supercooling $\Delta T = 20$ K. First, we approximate data obtained at the maximum aging time, $t_w = 8.0$ h, and find adjustable parameters Γ and W, which ensure the best fit of measurements. The quantities Γ and W are determined using the steepest-descent procedure. Afterwards, we fix the value $\Gamma = 1.21\ s^{-1}$ and match observations in tests with other waiting times using the only material parameter W. Figure 1 demonstrates fair agreement between experimental data and results of numerical simulation.

The same procedure of fitting is repeated for observations in relaxation tests with $\Delta T = 35$ K and $\Delta T = 50$ K. Figures 2 and 3 reveal that at all temperatures, eq. 39 ensures an acceptable approximation of experimental data.

The parameter W is plotted versus waiting time t_w in Figure 4, which shows that observations are fairly well approximated by the "linear" function

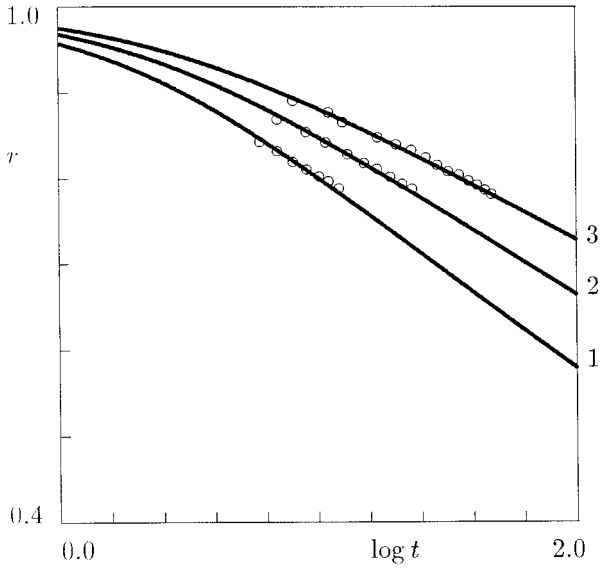

Figure 3 The ratio $r(t)$ versus time t (s) for PMMA in a tensile relaxation test after annealing at the temperature $T = T_g - 50$ K for a time t_w (h). Key: (circles) experimental data[51,52]; (solid lines) results of numerical simulation; (curve 1) $t_w = 2.0$; (curve 2) $t_w = 4.0$; (curve 3) $t_w = 8.0$.

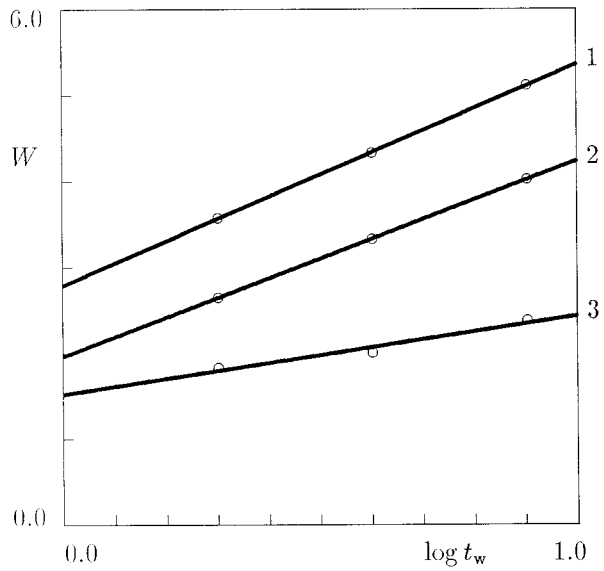

Figure 4 The dimensionless average energy of a CRR, W, versus waiting time, t_w, for PMMA in a tensile relaxation test at temperature T (K). Key: (circles) treatment of observations[51,52]; (solid lines) approximation of the experimental data by eq. 40. Key: (curve 1) $T = T_g - 20$, $a_0 = 1.5233$, $a_1 = 0.9135$; (curve 2) $T = T_g - 35$, $a_0 = 1.9633$, $a_1 = 2.2755$; (curve 3) $T = T_g - 50$, $a_0 = 2.7900$, $a_1 = 2.5745$.

$$W = a_0 + a_1 \log t_w \tag{40}$$

The adjustable parameters a_i in eq. 40 are determined by the least-squares technique. Equation 40 reflects the so-called logarithmic kinetics of structural recovery typical of polymeric glasses.[48]

The parameter a_1 (that characterizes the apparent rate of aging in eq. 40) and the rate of relaxation Γ are plotted versus temperature T in Figures 5 and 6. The apparent rate of aging, a_1, increases with the degree of supercooling ΔT. Experimental data are approximated by the linear function

$$a_1 = A\Delta T \tag{41}$$

where the coefficient A is found by the least-squares algorithm. The growth of the apparent rate of aging with ΔT is in agreement with experimental data in calorimetric tests (see, e.g., refs. 23, 24, 25), which demonstrate an increase in the rate of structural recovery with the degree of supercooling.

The rate of relaxation Γ decreases with ΔT (in agreement with the theory of thermally activated processes). The dependence $\Gamma = \Gamma(T)$ is fairly well approximated by the linear function

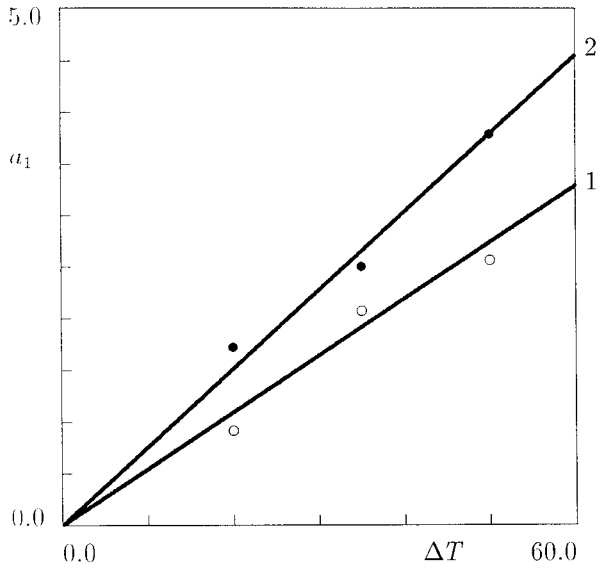

Figure 5 The dimensionless coefficient a_1 versus the degree of supercooling ΔT (K) in a tensile relaxation test. Key: (circles) treatment of observations[51,52]; (solid lines) approximation of the experimental data by eq. 41; (curve 1) PMMA, $A = 0.0548$; (curve 2) SAN, $A = 0.0759$.

$$\Gamma = \gamma_0 - \gamma_1 \Delta T \tag{42}$$

where the adjustable parameters γ_i are found using the least-squares algorithm.

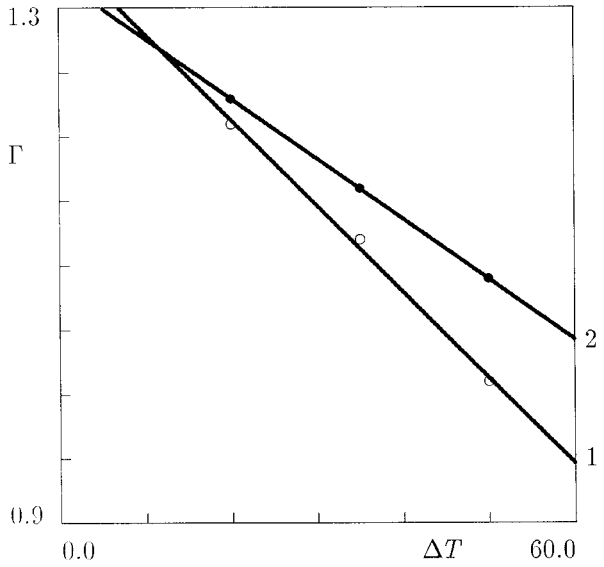

Figure 6 The rate of relaxation Γ (s^{-1}) versus the degree of supercooling ΔT (K) in a tensile relaxation test. Key: (circles) treatment of observations[51,52]; (solid lines) approximation of the experimental data by eq. 42; (curve 1) PMMA, $\gamma_0 = 1.3467$, $\gamma_1 = 0.0067$; (curve 2) SAN, $\gamma_0 = 1.3233$, $\gamma_1 = 0.0047$.

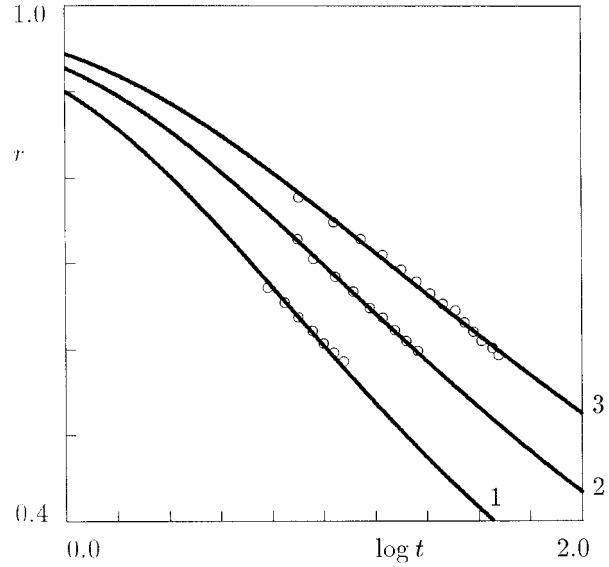

Figure 7 The ratio $r(t)$ versus time t (s) for SAN in a tensile relaxation test after annealing at the temperature $T = T_g - 20$ (K) for a time t_w (h). Key: (circles) experimental data[51,52]; (solid lines) results of numerical simulation; (curve 1) $t_w = 2.0$; (curve 2) $t_w = 4.0$; (curve 3) $t_w = 8.0$.

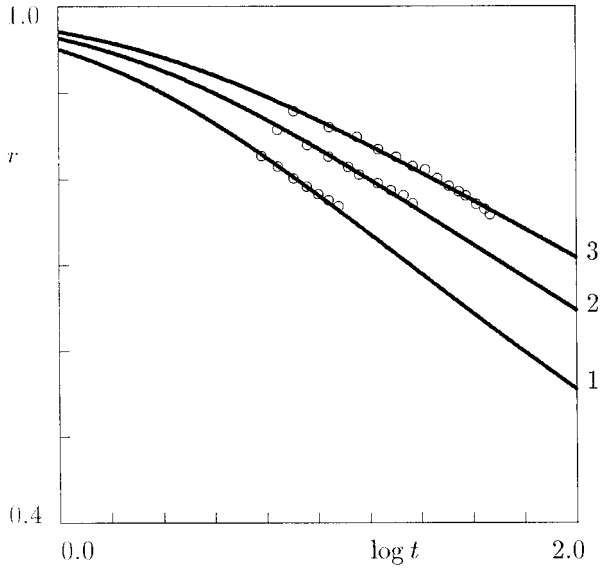

Figure 8 The ratio $r(t)$ versus time t (s) for SAN in a tensile relaxation test after annealing at the temperature $T = T_g - 35$ (K) for a time t_w (h). Key: (circles) experimental data[51,52]; (solid lines) results of numerical simulation; (curve 1) $t_w = 2.0$; (curve 2) $t_w = 4.0$; (curve 3) $t_w = 8.0$.

We proceed with fitting observations in tensile relaxation tests for poly(styrene-*co*-acronitrile) at various temperatures T below the glass transition point $T_g = 94$°C. A description of specimens and the experimental data can be found in Mijovic and co-workers.[51,52] We employ the same procedure of matching experimental data as for poly(methyl methacrylate): at each temperature T, we first approximate the relaxation curve corresponding to the maximum waiting time after annealing. Fitting of this curve provides the relaxation rate Γ, which is used without changes in matching experimental data at other waiting times t_w (each relaxation curve is approximated by using the only adjustable parameter, W).

The results in Figures 7–9 demonstrate fair agreement between observations and results of numerical simulation. The parameter W is plotted versus aging time t_w in Figure 10, which shows that eq. 40 correctly predicts experimental data. The apparent rate of aging, a_1, and the rate of relaxation, Γ, are depicted in Figures 5 and 6, which reveal that phenomenological eqs. 41 and 42 adequately describe the effect of temperature on the rates of structural, a_1, and mechanical, Γ, relaxations.

We proceed with the approximation of experimental data in dynamic torsional tests on poly(vinyl acetate) at two temperatures T in the close vicinity of the glass transition temperature ($T_g = 35$°C). For a description of the experimental

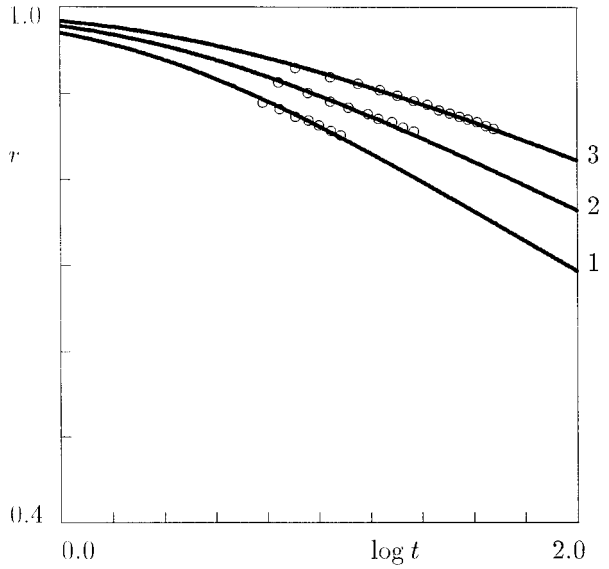

Figure 9 The ratio $r(t)$ versus time t (s) for SAN in a tensile relaxation test after annealing at the temperature $T = T_g - 50$ (K) for a time t_w (h). Key: (circles) experimental data[51,52]; (solid lines) results of numerical simulation; (curve 1) $t_w = 2.0$; (curve 2) $t_w = 4.0$; (curve 3) $t_w = 8.0$.

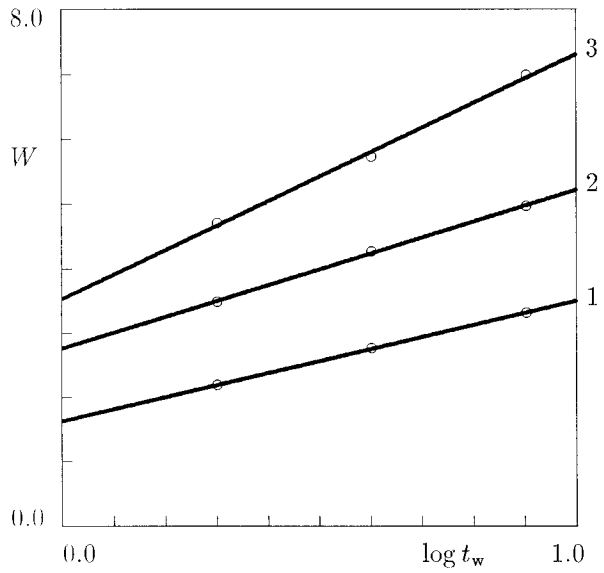

Figure 10 The dimensionless average energy of a CRR, W, versus waiting time, t_w, for SAN in a tensile relaxation test at temperature T (K). Key: (circles) treatment of observations[51,52]; (solid lines) approximation of the experimental data by eq. 40; (curve 1) $T = T_g - 20$, $a_0 = 1.6300$, $a_1 = 1.8769$; (curve 2) $T = T_g - 35$, $a_0 = 2.7633$, $a_1 = 2.4582$; (curve 3) $T = T_g - 50$, $a_0 = 3.5300$, $a_1 = 3.7870$.

procedure, we refer to Kovac et al.[19] First, we fit observations obtained at the maximum waiting time and determine adjustable parameters G_0 (an analog of the initial Young modulus for shear deformation), Γ, and W. Given an initial shear modulus G_0, the quantities Γ and W are determined by the steepest-descent procedure. The parameter G_0 is found using the least-squares algorithm. Afterwards, we fix the rate of relaxation Γ and proceed matching observations at other waiting times by employing only two adjustable parameters, G_0 and W. The results in Figure 11 demonstrate excellent agreement between results of numerical simulation and experimental data. The dimensionless parameter W is plotted versus waiting time t_w in Figure 12, which shows that phenomenological relation (eq. 40) fairly well approximates observations. The dependence of the initial shear modulus G_0 on waiting time t_w is depicted in Figure 13. This figure evidences that evolution of the initial shear modulus with waiting time is adequately predicted by the logarithmic law

$$G_0 = b_0 + b_1 \log t_w \tag{43}$$

where the adjustable parameters b_i are found by the least-squares algorithm.

CONCLUSIONS

A model has been developed for the effect of physical aging on the linear viscoelastic response of amorphous glassy polymers. Constitutive equations are derived that combine the theory of cooperative relaxation with the coarsening concept for structural recovery. Stress-strain relations are applied to fit experimental data for poly(methyl methacrylate) and poly(styrene-*co*-acronitrile) in tensile relaxation tests and for poly(vinyl acetate) in torsional dynamic tests at various temperatures in the sub-T_g region. Fair agreement is demonstrated between results of numerical simulation and observations. The following conclusions are drawn:

1. The time-aging time principle of superposition is not needed for the approximation of experimental data in mechanical tests on aged specimens.

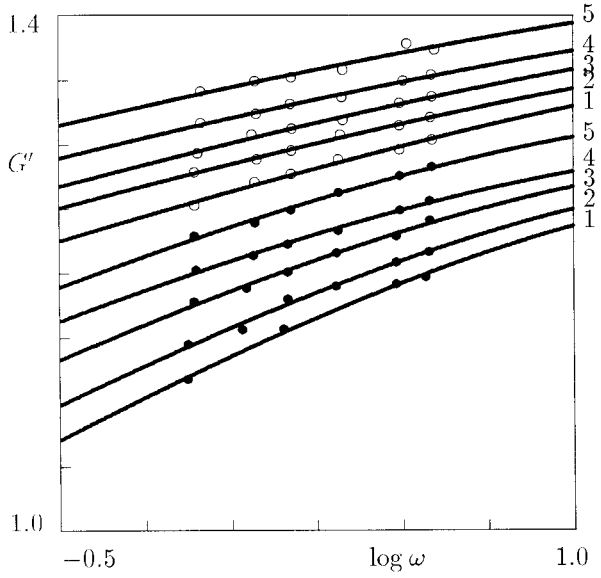

Figure 11 The storage modulus G' GPa versus frequency ω (rad/s) for PVAc in a torsional dynamic test after annealing for a time t_w (min) at a temperature T (°C). Key: (circles) experimental data[19]; (unfilled circles) $T = 20.0$; (filled circles) $T = 30.0$; (solid lines) results of numerical simulation with $\Gamma = 736.0$ s^{-1} ($T = 20.0$) and $\Gamma = 63.0$ s^{-1} ($T = 30.0$); (curve 1) $t_w = 50.0$; (curve 2) $t_w = 100.0$; (curve 3) $t_w = 200.0$; (curve 4) $t_w = 400.0$; (curve 5) $t_w = 1360.0$.

2. Excellent agreement between observations and results of numerical simulation is established, provided that the relaxation rate is independent of waiting time (which contradicts the theory of molecular mobility), whereas the average energy and the specific rigidity of a CRR increase with t_w (in agreement with the coarsening concept for structural recovery in glasses).
3. The annealing temperature T noticeably affects reformation of the energy landscape. The increase in the degree of supercooling, ΔT, results in an increase in the apparent rate of aging (in agreement with observations in dilatometric and calorimetric tests). Its effect on the evolution of initial elastic moduli is essentially weaker.
4. Phenomenological relations shown in eqs. 40 and 43 (which reflect the logarithmic kinetics of physical aging) fairly well approximate experimental data in static and dynamic mechanical tests.

Financial support by the Israeli Ministry of Science through grant 1202-1-00 is gratefully acknowledged.

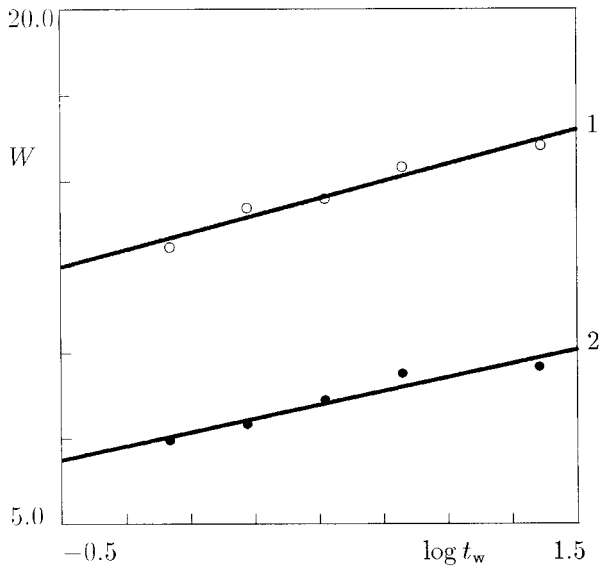

Figure 12 The dimensionless average energy of a CRR, W, versus waiting time, t_w, for PVAc at temperature T (°C). Key: (circles) treatment of observations[19]; (solid lines) approximation of the experimental data by eq. 40; (curve 1) $T = 20.0$, $a_0 = 13.5117$, $a_1 = 1.9997$; (curve 2) $T = 30.0$, $a_0 = 7.6821$, $a_1 = 1.6204$.

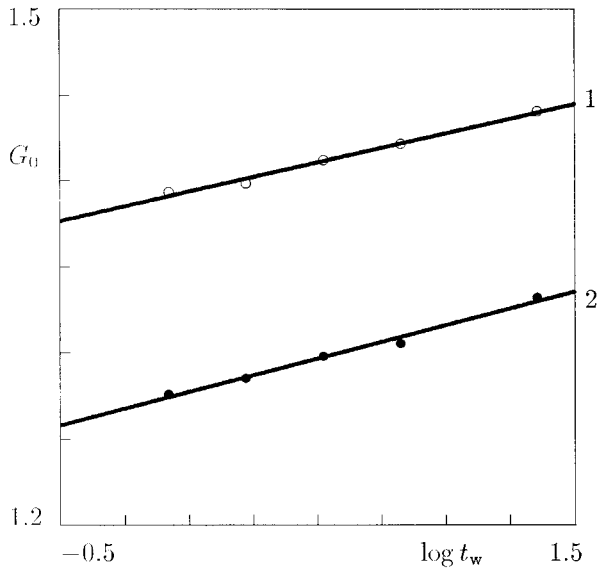

Figure 13 The initial shear modulus G_0 (GPa) versus waiting time, t_w, for PVAc at a temperature T (°C). Key: (circles) treatment of observations[19]; (solid lines) approximation of the experimental data by eq. 43; (curve 1) $T = 20.0$, $b_0 = 1.3937$, $b_1 = 0.0340$; (curve 2) $T = 30.0$, $b_0 = 1.2774$, $b_1 = 0.0386$.

REFERENCES

1. Donth, E.-J. Relaxation and Thermodynamics in Polymers: Glass Transition; Akademie Verlag: Berlin, 1992.
2. Matsuoka, S. Relaxation Phenomena in Polymers, Hanser-Verlag: Munich, 1992.
3. Debenedetti, P. G. Metastable Liquids: Concepts and Principles; Princeton University Press: Princeton, NJ, 1996.
4. Drozdov, A. D. Mechanics of Viscoelastic Solids; Wiley: Chichester, U.K., 1998.
5. McKenna, G. B. In Comprehensive Polymer Science; Booth, C.; Price, C., Eds.; Pergamon Press: Oxford, U.K., 1989; Vol. 2, p. 311.
6. Mijovic, J.; Nicolais, L.; D'Amore, A.; Kenny, J. M. Polym Eng Sci 1994, 34, 381.
7. Ediger, M. D.; Angell, C. A.; Nagel, S. R. J Phys Chem 1996, 100, 13200.
8. Bouchaud, J.-P.; Cugliandolo, L. F.; Kurchan, J.; Mezard, M. In Spin Glasses and Random Fields; Young, A. P., Ed.; World Scientific: Singapore, 1998; p. 161.
9. Struik, L. C. E. Physical Aging in Amorphous Polymers and Other Materials; Elsevier: Amsterdam, 1978.
10. Kobayashi, Y.; Zheng, W.; Meyer, E. F.; McGervey, J. D.; Jamieson, A. M.; Simha, R. Macromolecules 1989, 22, 2302.
11. Hill, A. J.; Katz, I. M.; Jones, P. L. Polym Eng Sci 1990, 30, 762.

12. Kluin, J.-E.; Yu, Z.; Vleeshouwers, S.; McGervey, J. D.; Jamieson, A. M.; Simha, R.; Sommer, K. Macromolecules 1993, 26, 1853.
13. Turnbull, D.; Cohen, M. H. J Chem Phys 1970, 52, 3038.
14. Cohen, M. H.; Grest, G. S. Phys Rev B 1979, 20, 1077.
15. Dyre, J. C. J Non-Cryst Solids 1998, 235–237, 142.
16. Macedo, P. B.; Litovitz, T. A. J Chem Phys 1965, 42, 245.
17. McKenna, G. B. J Non-Cryst Solids 1994, 172–174, 756.
18. Guerdoux, L.; Duckett, R. A.; Froelich, D. Polymer 1984, 25, 1392.
19. Kovacs, A. J.; Stratton, R. A.; Ferry, J. D. J Phys Chem 1963, 67, 152.
20. Greiner, R.; Schwarzl, F. R. Rheol Acta 1984, 23, 378.
21. Cowie, J. M. G.; Harris, S.; McEwen, I. J. Macromolecules 1998, 31, 2611.
22. Marshall, A. S.; Petrie, S. E. B. J Appl Phys 1975, 46, 4223.
23. Cowie, J. M. G.; Ferguson, R. Macromolecules 1989, 22, 2307.
24. Cowie, J. M. G.; Ferguson, R. Polymer 1993, 34, 2135.
25. Brunacci, A.; Cowie, J. M. G.; Ferguson, R.; McEwen, I. J. Polymer 1997, 38, 865.
26. Adam, G.; Gibbs, J. H. J Chem Phys 1965, 43, 139.
27. Sollich, P. Phys Rev E 1998, 58, 738.
28. Dyre, J. C. Phys Rev B 1995, 51, 12276.
29. Böhmer, R.; Hinze, G. J Chem Phys 1998, 109, 241.
30. Diezemann, G.; Mohanty, U.; Oppenheim, I. Phys Rev E 1999, 59, 2067.
31. Tanaka, H. J Phys: Condens Matter 1999, 11, L159.
32. Fisher, E. W. Physica A 1993, 201, 183.
33. Fisher, E. W.; Donth, E.; Steffen, W. Phys Rev Lett 1992, 68, 2344.
34. Arndt, M.; Stannarius, R.; Groothues, H.; Hempel, E.; Kremer, F. Phys Rev Lett 1997, 79, 2077.
35. Rizos, A. K.; Ngai, K. L. Phys Rev E 1999, 59, 612.
36. Mermet, A.; Duval, E.; Etienne, S.; G'Sell, C. Polymer 1996, 37, 615.
37. Bouchaud, J. P. J Phys I France 1992, 2, 1705.
38. Roland, C. M.; Santangelo, P. G.; Ngai, K. L. J Chem Phys 1999, 111, 5593.
39. Palmers, R. G. Adv Phys 1982, 31, 669.
40. Goldstein, M. J Chem Phys 1969, 51, 3728.
41. Alberici-Kious, F.; Bouchaud, J.-P.; Cugliandolo, L. F.; Doussineau, P.; Levelut, A. Preprint cond-mat/0003047.
42. Yoshino, H.; Lemaitre, A.; Bouchaud, J.-P. Preprint cond-mat/0009152.
43. Drozdov, A. D. Chem Phys Lett 2000, 327, 54.
44. Arkhipov, V. A.; Bässler, H. J Phys Chem 1994, 98, 662.
45. Monthus, C.; Bouchaud, J.-P. J Phys A 1996, 29, 3847.
46. Drozdov, A. D. Comput Mater Sci 1999, 15, 422.
47. Drozdov, A. D. Comput Mater Sci 2000, 18, 48.
48. Gibbs, M. R. J.; Evetts, J. E.; Leake, J. A. J Mater Sci 1983, 18, 278.
49. Khonik, V. A. Phys Stat Sol A 2000, 177, 173.
50. Robertson, R. E. J Polym Sci: Polym Symp 1978, 63, 173.
51. Mijovic, J.; Devine, S. T.; Ho, T. J Appl Polym Sci 1990, 39, 1133.
52. Ho, T.; Mijovic, J.; Lee, C. Polymer 1991, 32, 619.